

## Self-irradiation effects in plutonium alloys

N. Baclet<sup>a,\*</sup>, B. Oudot<sup>b</sup>, R. Grynszpan<sup>c</sup>, L. Jolly<sup>a</sup>, B. Ravat<sup>a</sup>,  
P. Faure<sup>a</sup>, L. Berlu<sup>a</sup>, G. Jomard<sup>d</sup>

<sup>a</sup> CEA-Centre de Valduc, F-21120 Is sur Tille, France

<sup>b</sup> Lawrence Livermore National Laboratory, Livermore, CA 94551, USA

<sup>c</sup> ITG, F-75008 Paris, France

<sup>d</sup> CEA-Centre Ile de France, F-91680 Bruyères le Châtel, France

Received 28 June 2006; received in revised form 25 October 2006; accepted 27 October 2006

Available online 11 December 2006

### Abstract

The plutonium  $\alpha$ -decay leads to the formation of numerous defects, which affect physical properties. This work presents swelling measured both at the macroscopic and microscopic scales on  $\delta$ -Pu alloys, together with a characterization of defects by positron annihilation spectroscopy (PAS). Swelling seems to depend on deltagen element and/or on  $\alpha$ -decay rate, and differences are observed between macroscopic and microscopic swelling. PAS results suggest that the concentration of vacancy clusters increases at the early stages of aging. Simulation of displacement cascades performed by molecular dynamics revealed a very long time (a couple of nanoseconds) to reach thermalization, contrary to what is observed in other fcc metals.

© 2006 Elsevier B.V. All rights reserved.

**Keywords:** Actinide alloys and compounds; Radiation effects; Crystal structure; Positron spectroscopies; Molecular dynamics simulation

### 1. Introduction

Plutonium remains the most peculiar element of the periodic table. It lies at the boundary between the light actinides (with delocalised 5f electrons) and the heavy actinides (with localised 5f electrons). This induces special behaviours such as, for instance, the occurrence of six allotropic phases transitions at ambient pressure associated with large volume changes. At room temperature, plutonium crystallises in the monoclinic phase ( $\alpha$ ) but can be stabilised in the fcc phase ( $\delta$ ) by adding “deltagen” elements such as aluminium, gallium, americium or cerium. The plutonium decay leads to the creation and recoil of uranium and helium ions, which produce defects through displacement cascades. These self-irradiation defects tend to change plutonium properties.

Complex electronic structure of pure and even more  $\delta$ -Pu alloys adds another difficulty since for example, modeling of displacement cascades using molecular dynamics requires specific interatomic potentials [1]. Moreover, the difficulty in handling

plutonium explains the lack of data on the properties of self-irradiation defects.

Self-irradiation phenomena in  $\delta$ -Pu alloys are then unique and understanding aging in plutonium alloys remains a real challenge that requires the development of very ambitious modeling and experiments, as detailed in the following.

First, the observed effects of aging on physical properties of different  $\delta$ -Pu alloys are presented. Predicting these effects, which is the following step, goes through their description at a very fine scale, which requires the coupling of modeling and experiments. A multi-scale approach, both experimental and theoretical, is then presented.

### 2. Experimental details

#### 2.1. Alloys studied

$\delta$ -Pu alloys stabilized with different deltagen elements (gallium and americium) were characterized. PuGa alloys were synthesized at CEA Valduc. After induction melting and cooling down to room temperature, a heat treatment at 733 K during 200 h under secondary vacuum was performed on the samples to homogenize the solute distribution. PuAm alloys were prepared at the Institute for Transuranium Elements by arc melting and were casted into copper moulds and then cooled down to room temperature. For all the  $\delta$ -Pu alloys mentioned,

\* Corresponding author. Tel.: +33 4 38 78 56 63; fax: +33 4 38 78 52 17.  
E-mail address: nathalie.baclet@cea.fr (N. Baclet).

X-ray diffraction (XRD) revealed  $\delta$ -monophased alloys. Rather sharp XRD peaks suggested a good homogeneity in solute distribution. This was confirmed on the PuGa alloys through quantitative concentration profiles determined by electron probe microanalysis.

## 2.2. Swelling measurements

Both types of swelling were investigated versus time, which is expressed hereafter in units of displacements per atom (dpa). For the PuGa alloys studied here, 1 dpa corresponds to about 10 years aging. Macroscopic swelling ( $\Delta L/L_{t=0}$ ) was measured by optical fibre Bragg grating sensor [2]. In order to be able to observe a significant change in swelling through the Bragg grating sensor, the fibre was carefully stuck in a groove of the sample [3]. The sample equipped with the optical fibre was then introduced in a furnace and this device was placed in glove box. The time dependence of the sample elongation was followed under isothermal conditions. Microscopic swelling was observed by XRD through the measurement of the change in variation of the lattice parameter versus time ( $\Delta a/a_{t=0}$ ). Experiments were performed both in laboratory (on a classical D8-Brüker diffractometer or on a rotating anode) and at European Synchrotron For Radiation Facility (ESRF, Grenoble).

## 2.3. The positron annihilation spectroscopy technique (PAS)

Depending on the sample depth to be probed, numerous techniques are available to study point defects in materials. However, due to radiotoxicity, rapid oxidation or nuclear stability of  $^{239}\text{Pu}$ , some techniques had to be dismissed, including: (i) transmission electron microscopy, requiring very thin samples (sensitive to oxidation), which precludes confinement, (ii) small angle neutron scattering, only applicable to  $^{242}\text{Pu}$  isotope, less fissible but not readily available and (iii) small angle X-ray scattering, as the defect contribution in the confinement could not easily be separated from that of the plutonium sample.

In contrast, PAS allowed remote detection (i.e., outside a glove box) of gamma photons resulting from positron annihilation, and hence the use of an easy sample confinement. A standard “sandwich” configuration consisting of a  $^{22}\text{Na}$  positron source inserted between two plutonium samples was confined in an aluminium box, which in turn was enclosed in a plexiglas box. These operations were done in a glove box. The sample holder was then sealed between two polymer sheets, ready for measurements on the lifetime spectrometer.

The basic principles of the related techniques have already been described long ago, for instance by West [4]. A positron implanted in the material is sensitive to the electronic density and hence to the presence of vacancy-type defects, which trap the thermalised positive probe and strongly affect its lifetime. In this study, we mainly used the positron lifetime technique, which in principle, can associate a specific lifetime component ( $\tau_i$ ) to a specific defect (trap) size or type  $i$ , with a contribution ( $I_i$ ) proportional to the defect concentration. For several types of traps, the mean lifetime can therefore be defined as:  $\tau_{\text{mean}} = \sum \tau_i I_i$ .

## 3. Experimental evidence of aging effects

### 3.1. Macroscopic and microscopic swelling

Swelling is often the most obvious consequence of radiation damage, whatever the material (fuel, irradiated steel, ...) and the scale of observation.

Few data have been published concerning the continuous following at room temperature of macroscopic swelling of  $\delta$ -Pu alloys. In this work, measurements were performed on a PuGa 2.2 at.% alloy. After a transient period, that lasted until  $\sim 0.1$  dpa, macroscopic swelling follows a linear trend. The latter part is attributed to helium bubbles [5], whereas two hypotheses are still proposed to explain the transient part: emergence of precipitate  $\text{Pu}_3\text{Ga}$  [6] and contribution of vacancies [7]. To go further, microscopic swelling was followed versus time.

Microscopic swelling was first reported in PuGa alloys by Chebotarev and Utkina [8], who indicated a saturation in swelling after about 2.5 years and a swelling at saturation that followed a positive linear trend with gallium content. In this work, microscopic swelling was carefully followed on fully homogenized PuGa alloys with several gallium contents (1.9, 3.4 and 6 at.%), measurements were performed in laboratory on a D8-Brüker diffractometer. Lattice parameter starts to

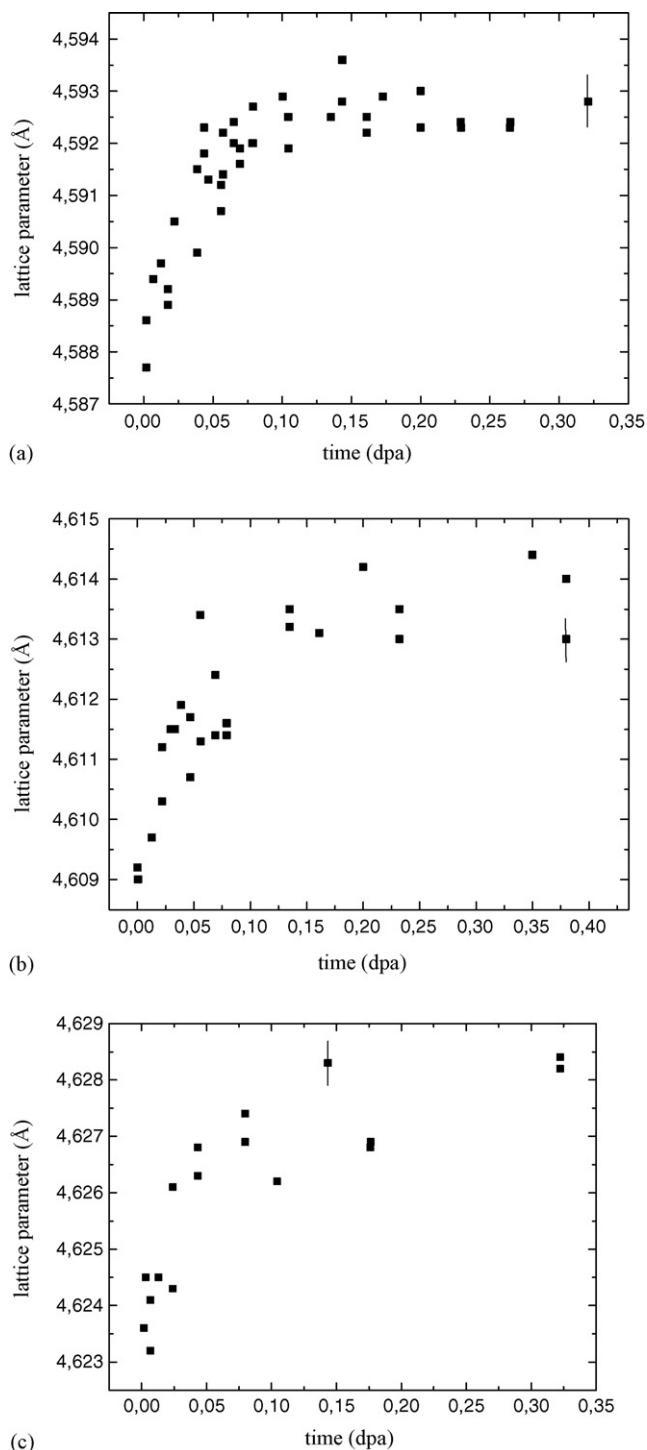


Fig. 1. Change in lattice parameter vs. time for  $\delta$ -PuGa alloys: (a) 6 at.%, (b) 3.4 at.% and (c) 1.9 at.%.

Table 1  
Characteristics of the  $\delta$ -PuAm alloys studied

Am content (at.%)	$\alpha$ -Decay rate ( $\text{s}^{-1} \text{g}^{-1}$ )	Number of $\alpha$ -decays $\text{g}^{-1}\text{a}$	$^{237}\text{Np}$ content <sup>a</sup> (at.%)	U content <sup>a</sup> (at.%)
0	$2.6 \times 10^9$	–		
8	$12.7 \times 10^9$	$4 \times 10^{17}$	0.1	0.028
15	$21.2 \times 10^9$	$6.7 \times 10^{17}$	0.18	0.026
18	$25 \times 10^9$	$7.9 \times 10^{17}$	0.21	0.026
24	$32.4 \times 10^9$	$10.2 \times 10^{17}$	0.28	0.025

<sup>a</sup> When characterization of the samples done.

increase immediately after casting, and tends to saturate after only 0.08 dpa, as shown in Fig. 1 for the three PuGa alloys [9]. XRD data revealed a large amount of scatter compared to dilatometric data. This can be explained by the difficulty in fitting the XRD pattern with an ideal face centered cubic structure whereas the cubic structure of  $\delta$ -PuGa alloys is distorted [9]. The lower the gallium content, the stronger the lattice distortion. This led to a limited accuracy for the lattice parameter and to the strong scatter observed. Absolute swelling at saturation ( $\Delta a = a^{\text{sat}} - a^{t=0}$ ) does not depend on gallium content for the range of gallium content studied, and  $\Delta a \sim 4.5 \times 10^{-3} \text{ \AA}$ . The relative swelling ( $\Delta a/a^{t=0}$ ) increases with gallium content since the higher the gallium content, the lower the lattice parameter  $a^{t=0}$ .

Change in lattice parameter with time was also determined on several 7-year old  $\delta$ -PuAm alloys ( $^{241}\text{Am}$  content ranging from 8 to 24 at.%). XRD measurements were performed both in laboratory on a rotating anode and at ESRF, and data were similar. Due to the limited size of the samples (mass  $\sim 5 \mu\text{g}$ ), self-heating of the samples was negligible. As only aged samples were available, the reference lattice parameter was deduced from measurement on the aged samples after a heat treatment of 6 h at  $450^\circ\text{C}$  which annealed the structural defects such as vacancies, interstitials, but which did not affect the chemical defects such as uranium and neptunium. Due to the short half-time period of  $^{241}\text{Am}$ , self-irradiation defects appeared at a higher rate in the PuAm alloys compared to the PuGa alloys, as indicated in Table 1. This means that the equivalent age of each PuAm sample was different regarding dpa. Lattice swelling reached saturation after about 0.08 dpa which corresponds to  $5.4 \times 10^{16} \alpha$ -decays  $\text{g}^{-1}$ , as observed for PuGa alloys; one could then assume that saturation was reached for

all the PuAm alloys studied. For PuAm alloys with 8, 15 and 18 at.% Am, the swelling of lattice parameter was lower than for PuGa alloys, and the PuAm 24 at.% alloy even showed a contraction with aging, as presented on Fig. 2. The different trend in lattice swelling for PuAm alloys could be partially attributed to the difference in chemical composition, and especially to the neptunium content, as indicated in Table 1. The rate of  $\alpha$ -decay, which is different for the PuAm alloys and between PuAm and PuGa alloys (see Table 1) could also influence the amplitude of swelling, as already observed for other irradiated materials [10]. More precisely, we can consider the so-called “peak swelling” curve, which describes the amplitude of swelling versus temperature at which the sample ages. For all the  $\delta$ -Pu alloys studied, we assume that the sample aged at room temperature. A change in the americium content, that is a change in the rate of  $\alpha$ -decay can shift the peak-swelling curve and then modify the amplitude of swelling for the different alloys.

Whereas, both PuGa and PuAm alloys have the same crystallographic structure, their behaviour regarding microscopic swelling during aging appears significantly different and is not fully understood yet. Moreover, microscopic and macroscopic swellings of PuGa alloys show a different behaviour versus time. Whereas, after a transient period, microscopic swelling saturates (after about 0.08 dpa), macroscopic swelling follows a linear trend. This suggests that swelling might be the sum of several contributions that affect differently macroscopic and microscopic scales. This reveals that it remains necessary to better understand the origin of swelling, which requires a fine description of the defects formed during aging. Characterization of defects at early stages was then investigated by PAS.

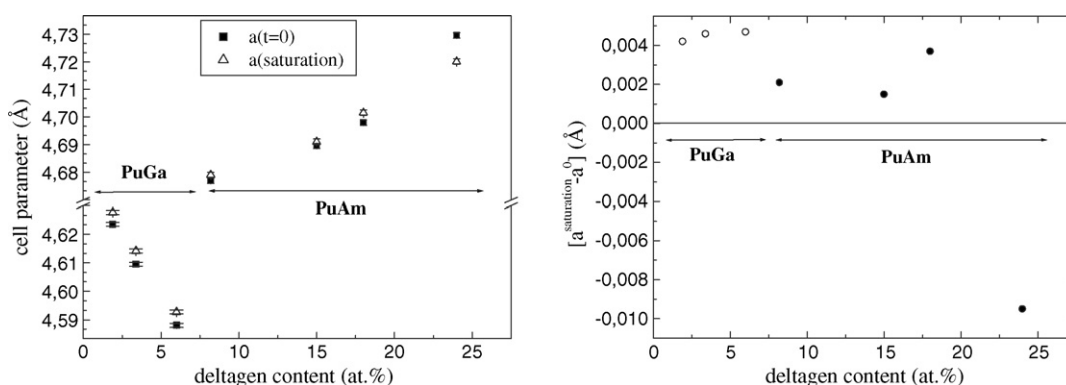


Fig. 2. Lattice parameter for aged and annealed alloys (left) and difference in lattice parameter (right) for  $\delta$ -PuGa and  $\delta$ -PuAm alloys.

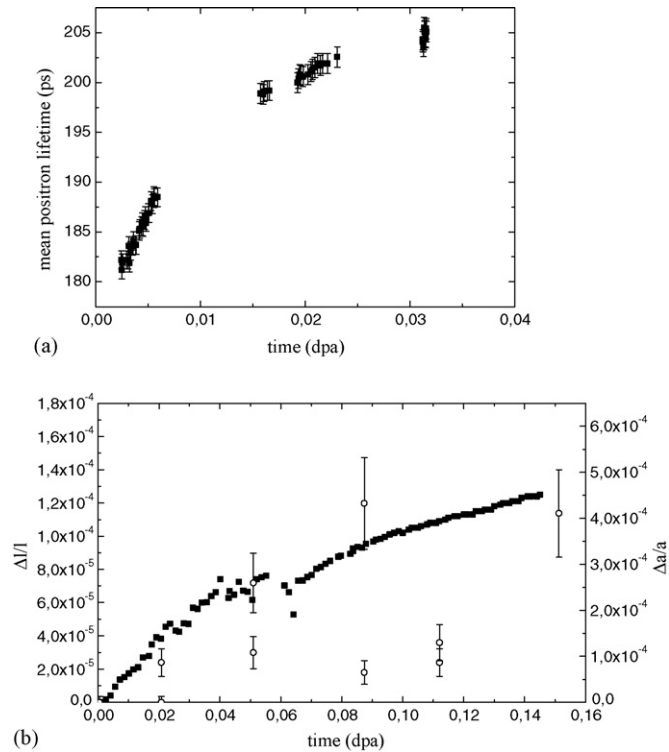


Fig. 3. Evolution vs. time, for a  $\delta$ -PuGa 1.9 at.% alloy: (a) mean positron lifetime and (b) macroscopic  $\Delta L/L$  (black squares) and microscopic  $\Delta a/a$  (open circles) swelling (right), measured by dilatometry and XRD, respectively.

### 3.2. Characterization of defects

Only the mean lifetime  $\tau_{\text{mean}}$  as deduced from positron annihilation spectroscopy is presented in Fig. 3, since analyses of lifetime spectra could not allow a reliable deconvolution into several possible components. While enough vacancy-type defects are produced (even at low dpa values) to ensure that all positrons are trapped, those with the largest trapping efficiency will provide the dominant contribution to the mean lifetime. The increase of  $\tau_{\text{mean}}$  can be associated with an increase in the concentration of vacancy clusters and/or an increase in size of vacancy-type defects. Microscopic swelling, as deduced from XRD, increases on the same period of time. As XRD is sensitive only to long-range order, a change in lattice parameter suggests that a sufficient number of (small) defects have been created, whereas a limited number of (large) defects would not affect lattice parameter but would deform the lattice, resulting in X-ray line broadening. The coupling of PAS and XRD measurements then suggests an increase in the concentration of vacancy clusters. PAS measurements at longer times are necessary to confirm this first interpretation and to follow the emergence of helium bubbles.

Even if the description of this first stage of defects creation is essential to understand further evolutions, it remains necessary to quantify the changes in physical properties, especially swelling, for much longer periods, for which samples are not available. A multi-scale (time and space) modeling of self-irradiation effects was therefore developed to predict the changes. The prime aim was to compare modeling and

experiments regarding the swelling data. Moreover, multi-scale modeling might unveil the presence of specific defects required for a more realistic assessment of aging phenomena, and in turn also suggest additional specific experiments for their characterization.

### 4. Aging multi-scale modeling

Aging involves different time and space scales which range from atomic and nanoseconds to macroscopic and years, and cannot be described by a single molecular simulation method. Consequently, a multi-scales approach, both in time and space, was developed to study self-irradiation damages by computer simulations. This approach combined molecular dynamics (MD) for the atomic scale, mesoscopic Monte Carlo (MC) and kinetic rate calculations (KR). The formation of primary defects was calculated using MD simulations of displacement cascades. Further diffusion and recombination process of the defects formed were studied with mesoscopic MC simulations. It must be noted that the input parameters of MC simulations were not only the number of defects formed during displacement cascade, but also spatial distribution of defects and their ability to form clusters; these characteristics could only be reached by MD computer simulations.

The success of the modeling lies in the ability of the interatomic potential to reproduce physical properties of plutonium (pure or alloyed). Ab initio calculations were used to determine properties such as elastic constants, bulk modulus and relative phase stability that were essential input data for the interatomic potential used for MD calculations [11].

Both uranium and the  $\alpha$  particles produced by plutonium decays give rise to lattice defects through displacement cascades. Most of these defects are due to uranium carrying a kinetic energy about 64 keV available for cascades [12]. The formation of primary defects following plutonium decay is obtained through MD simulations of displacement cascades due to uranium. Displacement cascades were calculated using MD with a progressive increase in the energy of the recoil atom.

First, results were obtained for 10 keV PKA energy in the  $\langle 1052 \rangle$  and  $\langle 1025 \rangle$  directions [13]. Both cascade behaviours were very similar. For the two directions, the ballistic phase lasted about 4 ps. About 4500 Frenkel pairs were created at the ballistic peak and approximately 1700 remained at 0.1 ns. The complete annealing of the cascade core was quite long putting in evidence that plutonium does not behave like any other fcc metals [14]. Computing the spatial expansion and repartition of defect microstructures reveal that, from the first stage, displacement cascades led to the formation of an amorphous core of 5 nm average radius with approximately 5000 Frenkel pairs. At the end of the defects recombination stage, which took place on a long time scale (a couple of nanoseconds), only a few interstitials remained out of the melting zone with an equal number of mono-vacancies within the melting zone. These results did not directly compare to PAS measurements since the time scale was much shorter here.

Further diffusion of the defects formed will be described with Monte Carlo approaches (kinetic and mesoscopic) that allow

to calculate swelling induced by the remaining defects, and to compare directly to experimental swelling. In parallel, a more phenomenological approach, based on kinetic rate equations has been developed and first results compared to experimental macroscopic swelling [7].

## 5. Conclusions

The complexity of self-irradiation effects in plutonium alloys required the development of a multi-scale approach, both theoretical and experimental, to better understand the origin of the changes in physical properties and even to predict aging effects at longer times. MD modeling revealed that results on plutonium are quite different from those on usual fcc metals and showed the necessity to use acceleration scheme to achieve these calculations. MC simulations must also be performed to describe higher time scales, and to compare directly with experimental data such as swelling.

As self-irradiation involves very tiny effects, dedicated techniques were developed to quantify these effects. Results were presented regarding swelling at macroscopic and microscopic scales on  $\delta$ -Pu alloys, suggesting a different contribution of defects depending on the scale and a possible influence of rate of  $\alpha$ -decay. PAS was proved to be a useful technique to identify

the defects formed at a very fine scale and further experiments are necessary.

## References

- [1] M.I. Baskes, Phys. Rev. B 62 (23) (2000) 15532.
- [2] V. Dewynter-Marty, P. Julia, A. Jacob, S. Rougeault, J. Boussoir, P. Ferdinand, 16th International Conference on Optical Fiber Sensors, OFS 16, Nara, Japan, 2003, p. 236.
- [3] P. Julia, in: G.D. Jarvinen (Ed.), Plutonium Futures—The Science, American Institute of Physical Education, 2003, p. 109.
- [4] R.N. West, in: P. Hautijärvi (Ed.), Positrons in Solids, Springer-Verlag, 1979, p. 89.
- [5] B.W. Chung, J.G. Tobin, S.R. Thompson, B.B. Ebbinghaus, Advances in Actinide Science, Royal Society Chemistry, 2006.
- [6] W.G. Wolfer, B. Oudot, N. Baclet, J. Nucl. Mater. 359 (2006) 185.
- [7] N. Gras, P. Julia, J. Alloys Compd., 2006.
- [8] N.T. Chebotarev, O.N. Utkina, Plutonium and Other Actinides, North Holland Publishing Company, Amsterdam, 1976, p. 559.
- [9] B. Ravat, B. Oudot, N. Baclet, submitted for publication.
- [10] J.L. Brimhall, E.P. Simonen, H.E. Kissinger, J. Nucl. Mater. 48 (1973) 339.
- [11] G. Robert, A. Pasturel, B. Siberchicot, Phys. Rev. B 68 (2003) 75109.
- [12] W.G. Wolfer, Los Alamos Sci. 26 (2000) 275.
- [13] L. Berlu, G. Jomard, G. Rosa, P. Faure, N. Baclet, F. Jollet, Materials Research Society Symposium Proceedings Series, 2006, p. 893.
- [14] D.J. Bacon, F. Gao, Y.U.N. Osetsky, J. Nucl. Mater. 276 (2000) 1.